International Journal of Heat and Mass Transfer 52 (2009) 2733–2739

Contents lists available at ScienceDirect

International Journal of Heat and Mass Transfer

journal homepage: www.elsevier.com/locate/ijhmt

Nucleate pool boiling of liquid methane and its natural gas mixtures

Maoqiong Gong *, Jia Ma, Jianfeng Wu, Yu Zhang, Zhaohu Sun, Yuan Zhou

Technical Institute of Physics and Chemistry, Chinese Academy of Sciences, Beijing 100190, China

ARTICLE INFO

Article history:
Received 16 June 2008
Received in revised form 24 December 2008
Available online 14 February 2009

Keywords:
Pool-boiling heat transfer
Liquid methane
Natural gas mixtures
Experimental measurement

ABSTRACT

An apparatus was designed and built for the study on pool-boiling heat transfer characteristics of pure and mixed fluids at cryogenic temperature. With this apparatus, extensive measurements were carried out to investigate the pool-boiling behaviors of pure methane and three binary mixtures of methane + ethane, methane + propane and methane + isobutane, as well as a multicomponent mixture of methane, ethane, propane and isobutane. The present measurements were performed in a descending heat flux procedure ranging from 250 kW/m^2 to 30 kW/m^2 at a fixed pressure of 0.13 MPa. Comprehensive measured data were presented in this paper, and also compared with some existing correlations. The deviations between the measured data and the predicted results locate within ±25% range.

1. Introduction

As a clean energy source, natural gas utilization is booming worldwide, and plays an important role in the economic and social sustainable development. The liquefied natural gas (LNG) is important in the worldwide natural gas trade because of its compact volume compared with its gas phase in the cases of oversea transport and huge amount storage. Many fundamental parameters such as thermodynamic properties as well as the heat and mass transfer data are crucial in designing and manufacturing LNG facilities. Among these, the nucleate pool-boiling heat transfer data of LNG are necessary parameters for design and optimization of LNG transportation, storage and gasification equipments. However, it is very difficult to find such measured pool-boiling heat transfer data of methane and its natural gas mixtures in open published literature, although the LNG industry has been developed for several decades. Bier and Lambert [1] reported their measurement of the pool-boiling heat transfer for some low-boiling substances such as methane, ethane, and argon, in which a horizontal copper cylinder with an outer diameter of 8 mm was used as the heat surface.

In this work, an apparatus was built to directly measure the pool-boiling heat transfer of the liquid methane and its natural gas mixtures. Extensive measurements on pool-boiling behaviors of the liquid methane and its mixtures with ethane, propane and isobutane were presented in the following sections. Comparisons with some existing correlations were also made.

2. Experiments

2.1. Experimental apparatus

The apparatus was designed to study the pool-boiling heat transfer of pure and mixed-refrigerants, which construction is quite similar to our former work [2,3]. A mixed-refrigerant Joule–Thomson cryocooler [4] was used to provide cooling capacity instead of liquid nitrogen for condensation of the boiling vapor. Fig. 1 shows the schematic diagram and photo of the experimental apparatus used in the present measurements. This experimental testing apparatus consists of a boiling vessel with a flat copper heat surface, a condensation system, two alternating-current (AC) power heaters, a refrigerant tank and a data acquisition system (Keithley, Model 2700, USA).

The boiling vessel is a vertical stainless-steel tube with an inner diameter of 75 mm and a height of 100 mm. Boiling takes place on the flat upper-end surface of a copper cylinder with a diameter of 20 mm, which is fixed on the bottom of boiling vessel. The heat surface was ordinarily lathed and then gritted with the 600 mesh sandpaper. An average roughness of 1.4 μm was obtained. Heat flux is supplied by a loop heater intertwined at the bottom of the copper cylinder. Different heating power can be supplied by adjusting an AC voltage regulator. The boiling vessel and heating unit were well insulated in a vacuum chamber. There are four platinum resistance thermometers installed in the copper cylinder at four separate points from the top to the bottom to obtain the temperature distributions. Another three thermometers are fixed separately in the liquid pool vessel to get the liquid temperature.

* Corresponding author. Tel./fax: +86 10 82543728.
E-mail address: gongmq@mail.ipc.ac.cn (M. Gong).

0017-9310/$ - see front matter © 2009 Elsevier Ltd. All rights reserved.
doi:10.1016/j.ijheatmasstransfer.2008.12.011

Nomenclature

D	mass diffusivity [$m^2\ s^{-1}$]
l	length [mm]
M	molar mass [kg $kmol^{-1}$]
n	number
p	pressure [MPa or Pa]
p_c	critical pressure [MPa or Pa]
R_a	surface roughness [μm]
q	heat flux [W m^{-2}]
T	temperature [K]
T_c	critical temperature [K]
u	standard uncertainty
U	expanded uncertainty
x	distance of the corresponding point from the heating surface [mm] composition of liquid phase [–]
y	vapor phase composition [–]

Greek symbols

α	heat transfer coefficient [W m^{-2} K^{-1}]
$\triangle T$	super heat [K]
$\triangle T_{bd}$	boiling range: the temperature difference between the dew and bubble points [K]
λ	thermal conductivity [W m^{-1} K^{-1}]

Subscripts

b	bubble point
d	dew point
i	the number of the temperature measurement point/ component number
id	ideal
l	liquid
w	wall

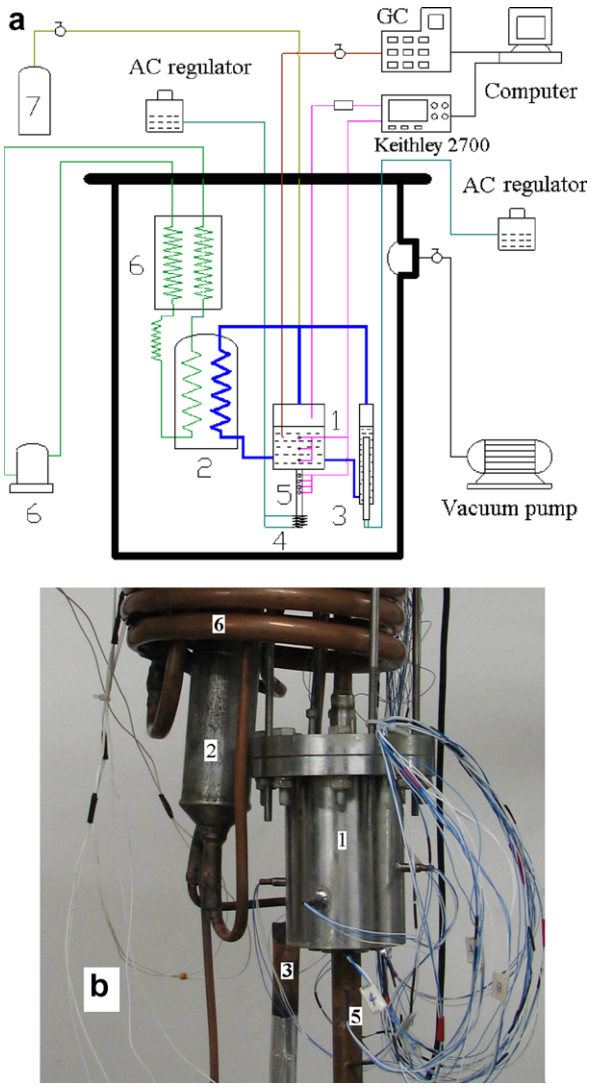

Fig. 1. The experimental apparatus, (a) schematic diagram and (b) photo of the system inside the vacuum chamber: (1) boiling vessel, (2) condenser, (3) accessorial electric heater, (4) loop heater, (5) copper cylinder, (6) cryocooler, (7) refrigerant tank.

2.2. Heat flux and surface temperature determination

An electrical heater was used to provide the heat flux in this work. Fig. 2 shows the locations of the four PT100 thermometers and the illustration of the temperature distribution in the mea-

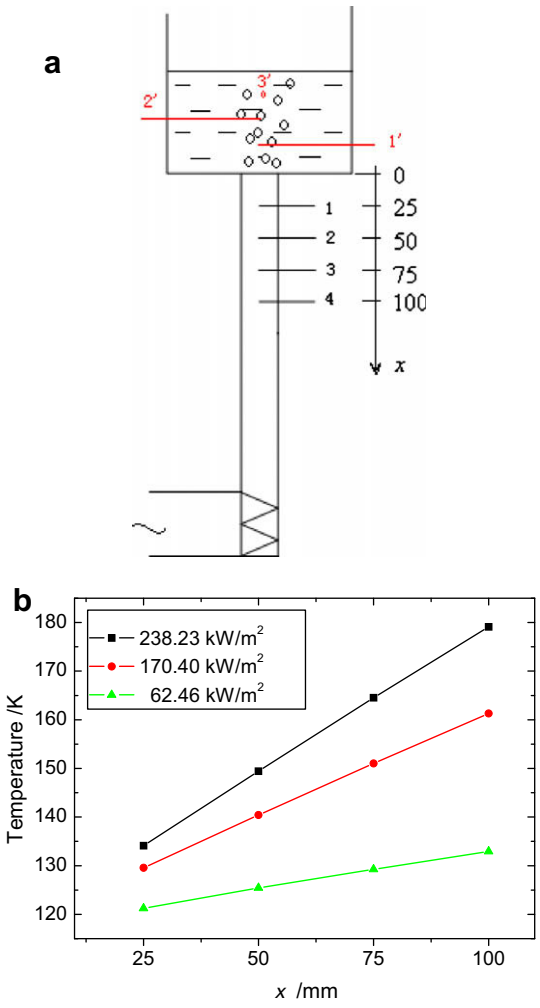

Fig. 2. (a) Schematic of the thermometers locations and (b) distribution of temperatures along the copper cylinder at different heat flux.

surement. An adiabatic condition can be ensured with the vacuum insulation. Therefore, the one-dimensional heat condition along the copper cylinder can be obtained. According to the Fourier Law, the following equation could be obtained:

$$q_i = \lambda_i (T_i - T_{i-1})/(x_i - x_{i-1}) \tag{1}$$

where x_i is the distance of the corresponding measurement point to the heating surface, and $i = 1,2,3,4$; T_i is the temperature, λ_i is the average thermal conductivity of copper cylinder between the i point and $i-1$ point, q_i is the heat flux between the two adjacent measurement points. As λ_i changes acutely with the temperature at low temperature range, it can be expressed as [5]:

$$\lg \lambda = \frac{a + cT^{0.5} + eT + gT^{1.5} + iT^2}{1 + bT^{0.5} + dT + fT^{1.5} + hT^2} \tag{2}$$

So, the average heat flux along the copper cylinder is

$$q = \left\{ \sum_{i=1}^{3} [\lambda_{i+1}(T_{i+1} - T_i)/(x_{i+1} - x_i)] \right\} \Big/ 3 \tag{3}$$

The heating surface temperature is

$$T_w = T_1 - \frac{q}{\lambda_1} x_1 \tag{4}$$

$$\text{where,} \quad \lambda_1 = \left(10^{\frac{a + cT_1^{0.5} + eT_1 + gT_1^{1.5} + iT_1^2}{1 + bT_1^{0.5} + dT_1 + fT_1^{1.5} + hT_1^2}} + 10^{\frac{a + cT_w^{0.5} + eT_w + gT_w^{1.5} + iT_w^2}{1 + bT_w^{0.5} + dT_w + fT_w^{1.5} + hT_w^2}} \right) \Big/ 2 \tag{5}$$

The constant parameters of a to i used in Eqs. (2) and (5) were taken from Ref. [5] and listed in Table 1.

2.3. Uncertainties analysis

The standard uncertainty (u_i) is the positive square root of the estimated variance u_i^2. The individual standard uncertainties are combined to obtain the expanded uncertainty (U), which is calculated from the law of propagation of uncertainty with a coverage factor [6].

Since the heat transfer coefficient (HTC) is obtained by the following equation:

$$\alpha = \frac{q}{T_w - T_l} \tag{6}$$

The uncertainty of HTC can be obtained with the following expression:

$$u(\alpha) = \sqrt{\left[\frac{\partial f(\alpha)}{\partial (q)} u(q)\right]^2 + \left[\frac{\partial f(\alpha)}{\partial (T_w)} u(T_w)\right]^2 + \left[\frac{\partial f(\alpha)}{\partial (T_l)} u(T_l)\right]^2} \tag{7}$$

Then the following task is to obtain uncertainty of each parameter. The temperatures are measured by means of PT100 type platinum electrical resistance thermometers. All PT100 thermometers were calibrated at temperatures ranging from 70 to 400 K with the accuracy of ±0.1 K. From Ref. [6], the uncertainty of temperature can be obtained as:

$$u(T) = \sqrt{\left[\frac{\partial (T)}{\partial x_1} u(x_1)\right]^2 + \left[\frac{\partial (T)}{\partial x_2} u(x_2)\right]^2 + \left[\frac{\partial (T)}{\partial x_3} u(x_3)\right]^2} \tag{8}$$

where $u(x_1)$ is the uncertainty of PT100 type platinum resistance thermometer itself; $u(x_2)$ is the uncertainty from the conversion between the temperature and the resistance measured by multimeter (Keithley, Model 2700 in this work); $u(x_3)$ is the uncertainty of the multimeter.

For the length measurement, the standard deviation of ten times length measurements is obtained as:

$$u(\bar{x}_i) = \sqrt{\frac{1}{n(n-1)} \sum_{i=1}^{n} (l_i - \bar{l})^2} \tag{9}$$

From Eq. (3), the uncertainty of heat flux can be expressed as:

$$u(q) = \sqrt{\begin{array}{l} \left[\frac{\partial f(q)}{\partial T_1} u(T_1)\right]^2 + \left[\frac{\partial f(q)}{\partial T_2} u(T_2)\right]^2 + \left[\frac{\partial f(q)}{\partial T_3} u(T_3)\right]^2 + \left[\frac{\partial f(q)}{\partial T_4} u(T_4)\right]^2 \\ + \left[\frac{\partial f(q)}{\partial l_1} u(l_1)\right]^2 + \left[\frac{\partial f(q)}{\partial l_2} u(l_2)\right]^2 + \left[\frac{\partial f(q)}{\partial l_3} u(l_3)\right]^2 + \left[\frac{\partial f(q)}{\partial l_4} u(l_4)\right]^2 \end{array}} \tag{10}$$

Finally, from above equations, the results of the uncertainties in this work were obtained and presented in Table 2.

3. Results and discussion

With the experimental apparatus described above, extensive measurements were carried out for pure methane and methane mixtures, which are listed in Table 3. Experimental measurements for each substance were repeated at least three times in the same condition to make sure that the data are reliable. Typical measured data are presented in the following sections. The heat flux was varied approximately between 30 kW/m^2 and 250 kW/m^2. All pool-boiling tests were taken at 0.13 MPa saturated conditions. The data were recorded consecutively starting at the largest heat flux and descending in intervals of approximate 25 kW/m^2. The descending heat flux procedure minimized the possibility of any hysteresis effects on the data.

3.1. Measured boiling data

3.1.1. Pure methane

The pool-boiling curve of pure methane was first measured. Fig. 3a shows the boiling curve of pure methane at 0.13 MPa. Seldom methane boiling data are available for comparison, especially those measured at similar heat surface and similar pressures. Bier and Lambert [1] have published their measurements on several substances including pure methane. In their article, a horizontal copper cylinder with an outer diameter of 8 mm was used as the heat surface, and pool-boiling heat transfer was measured at various pressures. For data of pure methane, one pressure condition of $p/p_c = 0.030$ ($p = 0.138$ MPa) is very close to this work ($p = 0.13$ MPa). Comparison is shown in Fig. 3b. It is clear that the tested heat flux of this work is larger than that of literature. Most

Table 2
The uncertainties of the experimental measurements.

$u(x_i)$/mm	$u(T_i)$/K	$u(T_w)$/K	$u(q)$/(kW/m^2)	$U(\alpha)$/%
0.01	0.1	0.11	0.54	14.2

Table 1
Constant parameters in Eqs. (2) and (5).

a	b	c	d	e	f	g	h	i
2.2154	−0.4761	−0.88068	0.13871	0.29505	0.02043	0.04831	0.001281	0.003207

Table 3
Substances measured in this work.

	Molar composition/%										
Methane	100	97	93	89	85	99	97	95	99	97	85
Ethane	/	3	7	11	15	/	/	/	/	/	11
Propane	/	/	/	/	/	1	3	5	/	/	3
Isobutane	/	/	/	/	/	/	/	/	1	3	1
T_b/K*	114.7	115.1	115.7	116.2	116.8	114.9	115.1	115.4	114.9	115.1	116.7
T_d/K*	114.7	141.2	149.9	155.1	159.0	164.2	176.5	183.0	185.9	199.8	192.6

* Bubble and dew point temperatures at 0.13 MPa, calculated by the PR equation of state [7].

data points obtained in this work locate at the extending line of Bier's data. By considering that different heat surface used, the results obtained in this work is acceptable. The heat surface condition is crucial to determine the boiling behavior even with the same fluid. The methane boiling curve was used as the base line in the following mixtures measurements. The boiling heat transfer coefficient is also presented in Fig. 3.

3.1.2. Binary mixtures

Ethane is another major component in the LNG except methane in most natural gas. Propane and isobutane are usually found in most natural gas. So the boiling behaviors of three binary mixtures of methane + ethane, methane + propane and methane + isobutane were studied in detail at the pressure of 0.13 MPa. Figs. 4–6 show the boiling curves of the three binary methane mixtures at various compositions, respectively. The measurement procedure and the variation of heat flux are quite similar to that of the pure methane.

It is obvious from Figs. 4–6 that increasing the molar concentration of the non-methane component significantly degrades the heat transfer performance of the methane mixtures since the wall super heat increases with an otherwise constant heat flux. For the same binary system, the super heat increases with the increase of the non-methane component concentration. For instance, from Fig. 4, the super heat varies from 4.5 to about 7 K at a heat flux of 200 kW/m^2 during the variation of the ethane molar concentration from 0% to 15%. As shown in Table 3, these binary mixtures are typical non-azeotropic mixtures with large boiling ranges, that is, large bubble and dew temperature differences. The decrease of heat transfer coefficient is due to the change of the mixture property and the mass transfer resistance near the boiling surface. An important characteristic of these non-azeotropic mixtures is that the component with low-boiling temperature, methane in this study, vaporizes first, while the other high-boiling point component almost remains liquid phase during the test. Therefore, in the boiling boundary layer, the concentration of the high-boiling component increases and contributes a lot to the mass transfer resistance. This deteriorates the boiling heat transfer [8]. This dete-

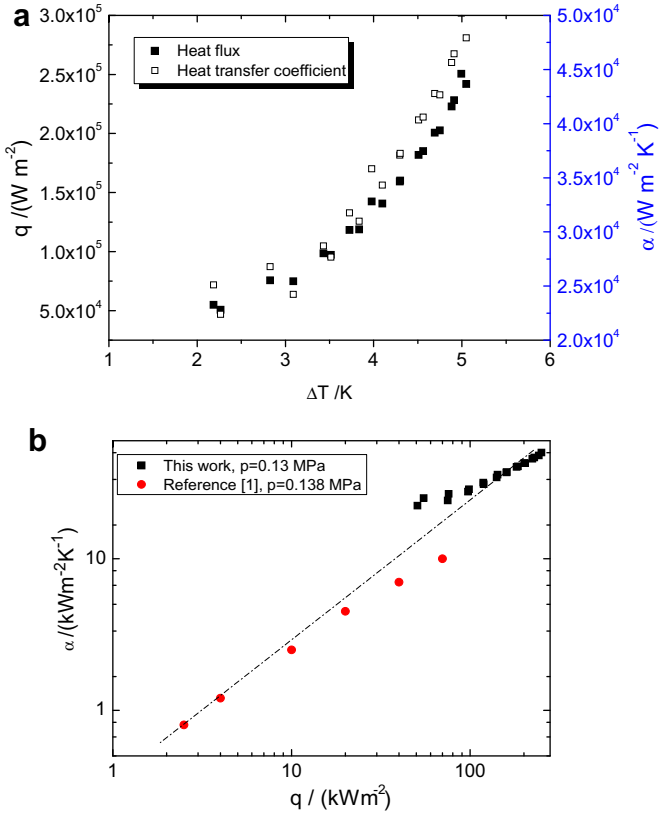

Fig. 3. Boiling curve of pure methane at 0.13 MPa. (a) Results of this work and (b) comparison with literature [1].

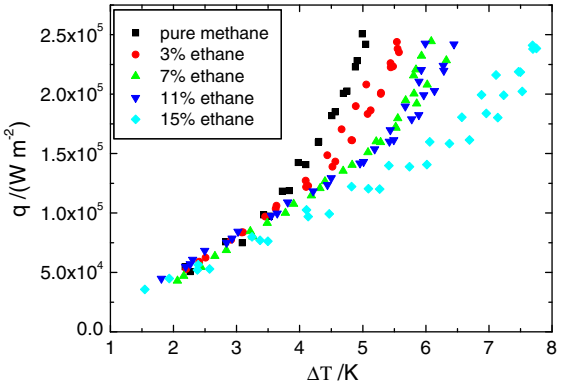

Fig. 4. Boiling curves of methane + ethane binary mixtures at various compositions.

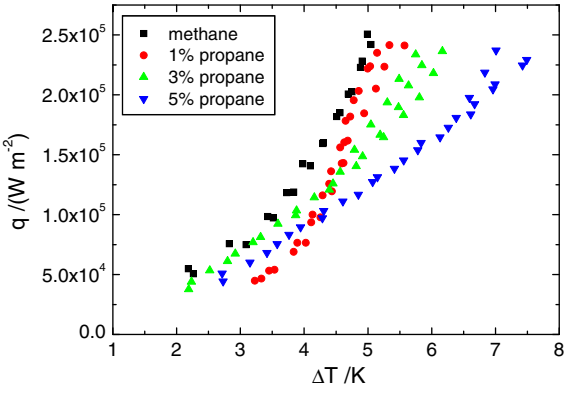

Fig. 5. Boiling curves of methane + propane binary mixtures at various compositions.

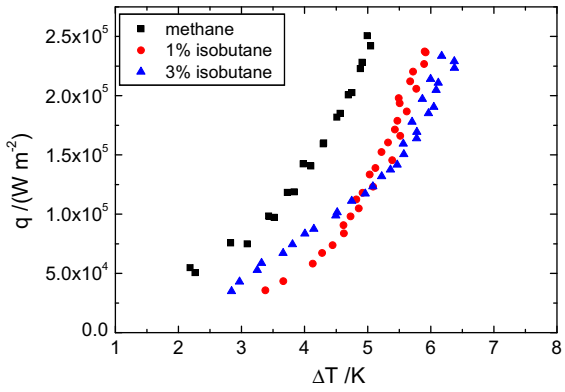

Fig. 6. Boiling curves of methane + isobutane binary mixtures at various compositions.

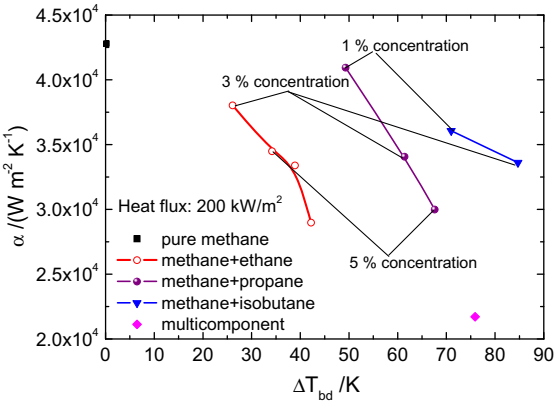

Fig. 8. Effect of boiling ranges on the HTCs.

rioration becomes obvious with the increase of the high-boiling component concentration.

However, exceptions were found in methane + propane and methane + isobutane systems. In these two binary systems, mixtures with 1% high-boiling component show some abnormal phenomena at the middle and low heat flux zone. That is, the mixtures with 1% concentration of high-boiling component show the largest super heat. The explanation of this phenomenon needs further study.

3.1.3. Multicomponent methane mixture

It is interesting to know the pool-boiling behavior of a real natural gas. The natural gas is a typical multicomponent non-azeotropic mixture, and its components and composition vary from different source well. In this study, a four-component methane mixture was prepared to stimulate a natural gas which has such composition as shown in Table 3. Fig. 7 shows the result of the experimental measurement. From the measured results, it is obvious that the boiling heat transfer performance deteriorates greatly compared with pure methane.

3.2. Variations of HTCs with boiling ranges

As already mentioned, the boiling range (ΔT_{bd}) is the temperature difference between the bubble and dew points. Fig. 8 shows the effect of ΔT_{bd} on the HTCs for above methane mixtures at the heat flux of 200 kW/m^2. It is clear from Fig. 8 that HTCs deteriorate substantially with the increase of ΔT_{bd} for these non-azeotropic mixtures. It can also be found that the deterioration of HTCs is much larger for those mixtures with wide boiling ranges (e.g. methane and isobutane mixtures) than those with narrow boiling ranges (e.g. methane and ethane mixtures) at same concentrations [9]. The multicomponent mixture has the lowest heat transfer coefficient among these substances, while its ΔT_{bd} is not the largest. The mass transfer in the multicomponent mixture boiling may contribute a lot to the heat transfer resistance.

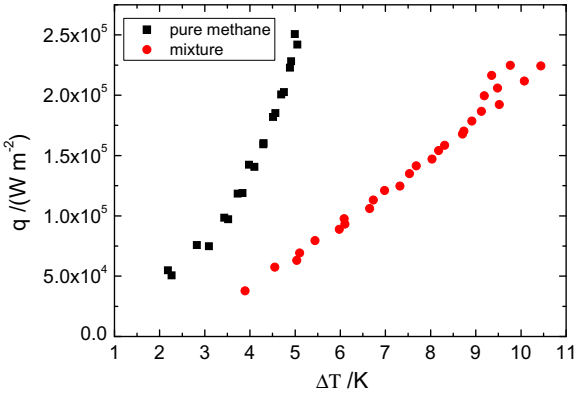

Fig. 7. Boiling curve of a multicomponent methane mixture.

3.3. Comparisons with existing correlations

Up to now, there are numerous correlations developed based on fluids physical properties and empirical parameters to describe the pool-boiling heat transfer behaviors. Most existing correlations were developed by correlating the corresponding experimental data with limited fluids and test conditions. So the extrapolation of those correlations sometimes is dangerous without experimental verification. There are few correlations available for pure methane and natural gas mixtures. In this section, some existing correlations were screened out, which are listed in Table 4. One correlation for pure methane was screen out from 12 correlations, and the other two correlations for binary mixtures were selected from 10 correlations, for details see Ref. [10]. Those three correlations can give acceptable agreement with the measured data. The comparisons between the predicted results and the measured data are presented in Figs. 9–12 for pure methane and its binary mixtures.

As for pure methane, Nishikawa's correlation [11], expressed as Eq. (11), shows good agreement with the measured data. The comparison of the predicted results with the measured data is presented in Fig. 9. For most data, the deviation between the predicted and the measured data locates within the ±25% range, while only a few data at low heat flux range exceed the −25% limits. For the binary mixture of methane and ethane, the comparison is shown in Fig. 10, in which Stephan's correlation [12] was used to get the predicted data. The deviation between the predicted and the measured data locates within the ±25% range for most data; while the deviation of some high ethane concentration data especially those at low heat flux exceed −25% limits.

For the other two binary mixtures of methane + propane and methane + isobutane system, the comparisons with predicted results by Calus' correlation [13] are shown in Figs. 11 and 12, respectively. From Fig. 12, only a few data of 5% propane concentration mixture exceed +25% limits. As for methane + isobutene system, all data locate within ±25% range. These correlations can give a quite acceptable agreement with the measured data obtained in this work. That is, those correlations listed in Table 4 can be used to predict the pool boiling of methane and its natural gas mixtures in some engineering application cases. From those results presented above, it can be found that the deviation between

Table 4
Some existing correlations.

Substances	Correlations	Eq.	Ref.
Pure methane	$\alpha = \frac{31.4P_c^{0.2}}{M^{0.1}T_c^{0.9}}(8R_a)^{0.2(1-P/P_c)}\frac{(P/P_c)^{0.23}}{[1-0.99(P/P_c)]^{0.5}}q^{0.8}$	(11)	[11]
Methane/ethane system	$\alpha = \frac{1}{1+1.53\lvert y-x\rvert(0.88+0.12p/10^5)}\left(\frac{\alpha_1\alpha_2}{\alpha_1x_2+\alpha_2x_1}\right)$	(12)	[12]
Methane/propane system	$\alpha = [1+\lvert y-x\rvert\left(\frac{\lambda_l}{D}\right)^{0.5}]^{-0.7}\left(\frac{\alpha_1\alpha_2}{\alpha_1x_2+\alpha_2x_1}\right)$	(13)	[13]
Methane/isobutene system	$\alpha = [1+\lvert y-x\rvert\left(\frac{\lambda_l}{D}\right)^{0.5}]^{-0.7}\left(\frac{\alpha_1\alpha_2}{\alpha_1x_2+\alpha_2x_1}\right)$	(13)	[13]

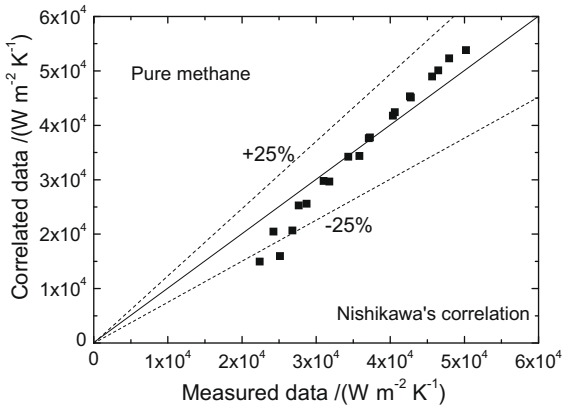

Fig. 9. Pure methane, comparisons with Nishikawa's correlation [11].

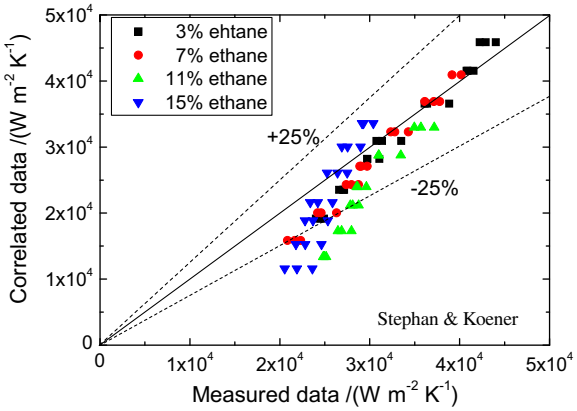

Fig. 10. Methane + ethane system, comparisons with Stephan's correlation [12].

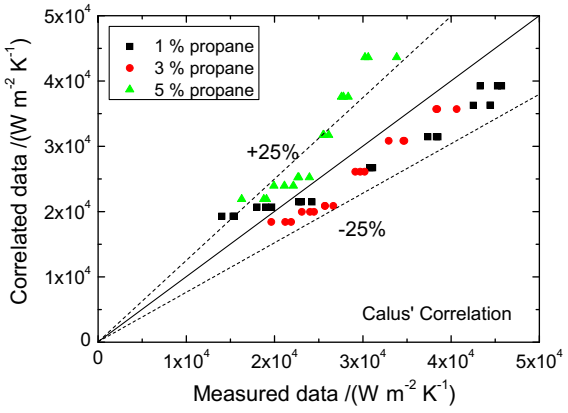

Fig. 11. Methane + propane system, comparisons with Calus' correlation [13].

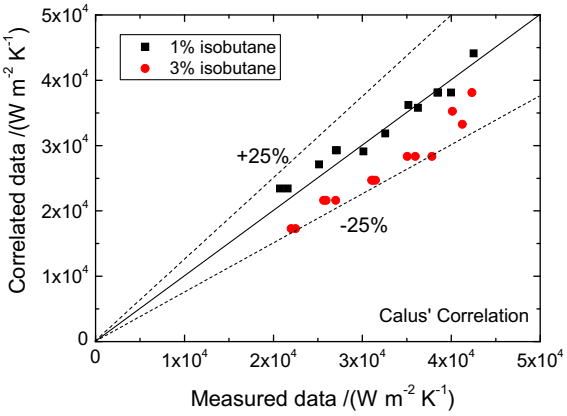

Fig. 12. Methane + isobutane system, comparisons with Calus' correlation [13].

the experimental data and predict results increases with the concentration increase of the non-methane component for these three binary mixtures. The pool-boiling heat transfer coefficient data of pure ethane were obtained from Refs. [3,14], and the pool-boiling heat transfer coefficient data of pure propane and isobutene were taken from Refs. [2,15].

4. Summary

In this work, an experimental apparatus was designed and built to investigate pool-boiling heat transfer characteristics for pure methane and its natural gas mixtures, which include three binary methane mixtures and a multicomponent methane mixture. The nucleate pool-boiling curves were measured under various heat fluxes from 30 to about 250 kW/m^2 at a fixed pressure of 0.13 MPa. From this study, the directly measured pool-boiling data for methane and its natural gas mixtures were obtained. These data will be useful in such LNG applications. The influence of the boiling range on boiling heat transfer was also analyzed. The HTCs deteriorate substantially with the increase of ΔT_{bd} for these non-azeotropic mixtures. Some typical semi-empirical correlations were screened out for comparison with the measured data. Those correlations can provide acceptable deviations for most data.

Acknowledgements

The authors acknowledge with gratitude the continued support received from the National Natural Sciences Foundation of China under the project number of 50890183.

References

[1] K. Bier, M. Lambert, Heat transfer in nucleate boiling of different low boiling substances, Int. J. Refrig. 13 (5) (1990) 293–300.
[2] Z. Sun, M.Q. Gong, J. Wu, Nucleate pool boiling heat transfer coefficients of pure HFC134a, HC290, HC600a, and their binary and ternary mixtures, Int. J. Heat Mass Transfer 50 (2007) 94–104.

[3] L. Zhang, M.Q. Gong, Y. Zhang, P. Li, J. Wu, L. Xu, Nucleate pool boiling heat transfer measurements of R170/R23 system, Int. Commun. Heat Mass Transfer 34 (2007) 277–284.
[4] M.Q. Gong, J. Wu, E. Luo, Performances of the mixed-gases Joule–Thomson refrigeration cycles for cooling fixed-temperature heat loads, Cryogenics 44 (2004) 847–857.
[5] N.J. Simon, E.S. Drexler, R.P. Reed, Properties of copper and copper alloys at cryogenic temperature, NIST Monogr. 177 (1992) 7–23.
[6] B.N. Taylor, C.E. Kuyatt, Guidelines for evaluation and expressing the uncertainty of NIST measurement results, NIST Tech. Note 1297 (1993) 1–20.
[7] ProII, User Manual V6.1, Simulation Science, Inc., 601 S. Valencia Ave., Brea, CA 92621, USA, 2003.
[8] R. Krupiczka, A. Rotkegel, Z. Ziobrowski, The influence of mass transport on the heat transfer coefficients during the boiling of multicomponent mixtures, Int. J. Therm. Sci. 39 (2000) 667–672.
[9] L.Q. Zhang, M.Q. Gong, J.F. Wu, L. Xu, Nucleate pool boiling heat transfer of binary mixtures with different boiling ranges, Exp. Heat Transfer 34 (2007) 277–284.
[10] Jia Ma, Experiment investigation on nucleate pool boiling heat transfer of methane and its hydrocarbon mixtures. Master degree thesis, Chinese Academy of Sciences, Beijing, 2008.
[11] K. Nishikawa, Y. Fujita, H. Ohat, S. Hidaka, Effect of the surface roughness on the nucleate boiling heat transfer over the wide range of pressure, in: Proceedings of the Seventh International Heat Transfer Conference, vol. 4, 1982, pp. 61–66.
[12] K. Stephan, M. Korner, A correlation for pool-boiling heat transfer, Chem. Eng. Technol. 41 (1969) 409–417 (in German).
[13] W.F. Calus, P. Rice, Pool boiling-binary liquid mixtures, Int. J. Heat Mass Transfer 17 (1974) 249–256.
[14] L.Q. Zhang, Experimental investigation on pool boiling heat transfer of new azeotropic mixed-refrigerants used in the cascade refrigeration temperature range. Ph.D. thesis, Shanghai Jiaotong University, Shanghai, 2006.
[15] Z.H. Sun, Experimental investigation on pool boiling heat transfer of multi-component mixed-refrigerants. Ph.D. thesis, Chinese Academy of Sciences, Beijing, 2005.